Key Engineering Materials
ISSN: 1662-9795, Vol. 926, pp 1725-1735
doi:10.4028/p-2ntbzl

Submitted: 2021-12-08
Revised: 2022-02-01
Accepted: 2022-02-02
Online: 2022-07-22

Impact of Die Coatings on Forming Conditions in Electromagnetic Embossing of Thin Sheet Metal

Björn Beckschwarte[1,4,a*], Julian Heidhoff[2,4,b], Lasse Langstädtler[1,3,4,c], Christian Schenck[1,3,4,d], Oltmann Riemer[2,3,4,e] and Bernd Kuhfuss[1,3,4,f]

[1]bime, Bremen Institute for Mechanical Engineering, Germany

[2]IWT, Leibniz Institute for Materials Engineering, Germany

[3]MAPEX Center for Materials and Processing, Germany

[4]University of Bremen, Germany

[a]beckschwarte@bime.de, [b]heidhoff@iwt.uni-bremen.de, [c]langstaedtler@bime.de, [d]schenck@bime.de, [e]riemer@iwt.uni-bremen.de, [f]kuhfuss@bime.de

Keywords: impulse forming, die manufacturing, coating

Abstract. In electromagnetic embossing, the interaction of the magnetic field and the induced current density results in body forces that enable the replication of optical microstructures into thin sheet metals. However, as the sheet metal is completely penetrated by the magnetic field, electromagnetic properties of the dies need to be considered in process design, as they influence the forming conditions by changing the field distribution, force vectors and eddy current densities. With die coatings like electroless nickel–phosphorus (NiP), the electromagnetic properties of the die change. Therefore, the effect of both - die substrate and coating material - was studied to find advantageous conditions for electromagnetic embossing. Within two-dimensional electromagnetic field simulation, the electromagnetic properties of coating and substrate material were varied in addition to the coating thickness. To validate the results, electromagnetic embossing experiments were carried out. Here, different dies were fabricated from aluminum (uncoated) and cold work steel with 200 µm and 400 µm thick electroless nickel–phosphorus coatings that were subsequently micro-structured in optical surface quality. It was demonstrated by numerical and experimental results that the coating and the substrate influence the electromagnetic embossing significantly in correspondence to their shielding behavior and field interaction due to electromagnetic properties and coating thickness.

Introduction

In electromagnetic forming, energy is transferred within a very short period of time by interaction of a pulsed electromagnetic field with the workpiece. This forming energy is usable for different manufacturing operations. These operations on tubular or sheet shaped workpieces include forming, joining, cutting, and embossing [1]. Especially the contactless transmission of energy benefits the embossing of optical and functional microstructures [2]. Furthermore, the electromagnetic embossing of thin sheet metal offers the advantage of body forces that act in the entire volume of the workpiece as the sheets are completely penetrated by the electromagnetic field. Golowin et al. [3] showed the replication of a diffraction grating image. Heidhoff et al. [4] replicated structures with retroreflective properties. Herrmann et al. [5] demonstrated the replication of structures with tribological properties.

In contrast to conventional mechanical based embossing operations, electromagnetic embossing can be integrated in other forming operations like further electromagnetic forming [6] or mechanical forming operations [7]. The high impulse energy enables microstructure replication in high quality and causes additional interactions between sheet metal and die. The high impulse energy generates high impact pressure on the die that causes die wear, which decreases the embossing quality. Risch et al. [8] concluded that the high contact pressure in combination with the workpiece motion promote die wear in electromagnetic forming. Herrmann et al. [5] showed that adhesive die wear in electromagnetic embossing can be reduced by DLC (diamond-like-carbon) coating. A higher amount of adhesion was observed when the die surface was prepared by polishing to receive a nearly optical

surface roughness. Thus, surface coatings are reasonable in particular for the embossing of optical surfaces and microstructure. Further coating systems based on Ti/TiAlN and TiAl/TiAlN for electromagnetic forming were discussed by Tillmann et al. [9] and compared in [10] with DLC coatings by impact tests and electromagnetic forming tests. During the forming tests, different wear behavior of the coatings was determined, which was assigned to the mechanical and tribological properties. In summary, to reduce die wear, a wide variety of coatings with different mechanical and electromagnetic properties can be used. Furthermore, coatings are required for further functions, such as providing a suitable surface for ultra-precision diamond machining with diamond tools [11]. However, further interactions must be considered.

Birdsall et al. described in [12] the effect of a counter pressure based on eddy currents in the die. These counter forces, like, the rebound-effect during workpiece impact [13], will reduce the forming accuracy. Th eddy currents arose when the electromagnetic field extended through the workpiece into the die due to partial shielding or by active induction with a secondary tool coil [14]. Comparable to the eddy current within the die is the provision of multiple tool coils, which are used, for example, to influence the draw-in [15] or the direction [16] and distribution of force [17].

Regarding eddy current in the die, Beckschwarte et al. showed how electromagnetic properties of dies can be used to affect the electromagnetic forming process by effecting field and current densities, force vectors and material forming behavior [18]. Therefore, based on the property gradient of the embossing dies by the coating, the interaction of coating and substrate material must be considered regarding the conditions of the embossing process of thin sheet metals. Thereby, the different combinations of electromagnetic properties of coating and substrate must be considered as well, where in particular the electric conductivity is of interest due to the counterforce. For this purpose, a two-dimensional simulation of the electromagnetic forming process was built with different electric conductivity of the coating and the substrate material. Furthermore, a variation of the coating thickness was carried out with the aim of determining the influence of coating thickness variations. The thickness can be varied in by the die design but may also change by the coating process or the machining microstructures in the coating layer. To validate the simulations, electromagnetic embossing experiments with uncoated aluminum and electroless nickel–phosphorus with 10-12 % phosphorus content (NiP) with coated steel dies with micro grooves in an optical surface were performed.

Setup

Simulation. The electromagnetic embossing process was simulated in Ansys Electronics Maxwell 2018.1. By using a single-conductor tool coil, the process was described in the plane normal to the current flow. The two-dimensional FEM-model consisted of tool coil, workpiece, die (coating and substrate) and the simulation region in which the calculation of the electromagnetic field took place (see Fig. 1 a). The die and the workpiece were electrically connected whereas the tool coil was insulated by a gap.

All elements were meshed with the Ansoft Tau Mesh method (triangular mesh) with a maximum mesh size of 0.5 mm. The mesh size was refined to 0.02 mm for the coating and the workpiece. The excitation of the tool coil was modelled according to an 1800 J current discharge curve I(t) of the capacitor bank measured in the experiments (see Fig. 1 b). The total simulation time t_s was set to 500 µs.

Within the simulation model, the electric conductivity σ – respectively the specific resistance $\rho = 1/\sigma$ – and the relative permeability μ_r of the substrate (material A) and the coating (material B) was varied. The electromagnetic properties, which are related to real materials that can be validated in experiments, are given in Tab. 1. Here, the dependence on temperature, heat treatment condition, frequency, and field strength (ferromagnetism), among other things, were not considered. Thus, the values can deviate to the material properties in the experiments. Further, a variation in material properties can be determined, especially for the properties of the NiP layers [19].

a)

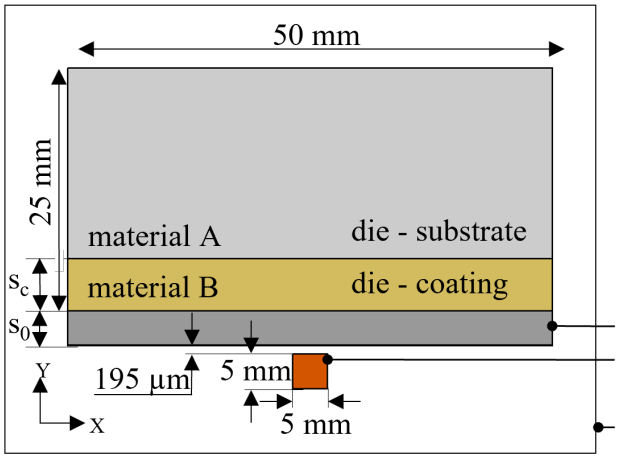

b)

$$I(t) = I_{max} * e^{-\delta * t} * \sin(2 * \pi * f * t)$$
$$I_{max} = 37.5\ kA$$
$$\delta = 5600$$
$$f = 14.5\ kHz$$

c)

	s_c	s_0
Minimum [µm]	100	100
Maximum [µm]	3000	1000
Steps [µm]	100	50

Fig. 1: Simulation model a) geometric properties b) current excitation c) variation of parameters s_c and s_0

For the NiP layer, the material values given in Tab. 1 were used due to the inability to measure the electric conductivity ρ and the relative permeability μ_r. The sheet metal thickness s_0 and coating thickness s_c were varied. The sheet metal thickness s_0 was varied from 100 µm to 1000 µm in 50 µm steps. The coating thickness s_c was varied from 100 µm to 3000 µm in 100 µm steps.

Tab. 1: Electromagnetic properties of used materials [20]

material	**part**	**electric conductivity** $\sigma\ [\frac{1}{\Omega m}]$	**relative permeability** μ_r **[-]**
AlCuMgPb	die (uncoated and coated substrate)	$38*10^6$	1.000021
90MnCrV8	substrate	$2*10^6$	300
NiP	coating	$14*10^6$	1
Al99.5	workpiece	$38*10^6$	1.000021
vacuum	die (with neutral properties)	0	1
Cu99	coil	$58*10^6$	0.999991

Furthermore, a wide variation of electric conductivity σ of the coating and the substrate was performed in simulations from a minimum value of an idealized insulator without electric conductivity $\sigma = 0\ ^1/_{\Omega m}$ to a maximum value related to the properties of copper with an electric conductivity $\sigma = 1*10^8\ ^1/_{\Omega m}$. Between these two extreme values, intermediate values were selected by means of logarithmic increments. Here, the relative permeability μ_r of both coating and substrate was set to 1. During this variation, the workpiece thickness s_c was 200 µm and the coating thickness s_c was 200 µm. Within all simulations, an aluminum (Al99.5) workpiece and a 5x5 mm² copper single-conductor tool coil was used.

The resulting impulse in y-direction of the workpiece $J_{y,w}$ over the total simulation time t_s was calculated as given by Eq. 1. Furthermore, the impulse difference $J_{d,y,w}$ compared to a die with neutral electromagnetic properties ($\sigma = 0\ ^1/_{\Omega m}$, $\mu_r = 1$) for substrate and coating was calculated (see. Eq. 2). As a consequence, by calculation of $J_{d,y,w}$, the impact of the die on the resulting impulse on the workpiece can be investigated isolated from the increase in impulse $J_{y,w}$ by the workpiece thickness s_0.

$$J_{y,w} = \int_0^{t_s} F_{y,workpiece} dt \tag{1}$$

$$J_{d,y,w} = J_{y,w} - J_{y,w}^{\text{neutral die}} \tag{2}$$

To consider the shielding of the electromagnetic field, the current penetration depth was calculated [21]. It is defined by the reduction of the current density in a body to approx. 37 % of the initial amplitude. The penetration depth p depends on the specific resistance ρ, the mathematic constant π, the relative permeability μ_r of the penetrated material, the vacuum permeability μ_0 and the frequency f of the electromagnetic field (see. Eq. 3).

$$p = \sqrt{\frac{\rho}{\pi * \mu_r * \mu_0 * f}} \tag{3}$$

Experimental. Simulations were validated by electromagnetic forming experiments. For all experiments, an impulse forming unit with a capacity of 100 µF and a maximum charge voltage of 6 kV was used. The experiments were performed with maximum charge voltage, which resulted in a charge energy of 1800 J. As tool coil, equivalent to the simulation model, a rectangular straight copper bar with the dimensions 5 x 5 mm² was isolated by a 195 µm thick polyimide layer. The combined discharge frequency of the forming system (forming unit and tool coil) was approx. 14.5 kHz. Rectangular aluminum (Al99.5) sheets with an outer dimension of 50 x 50 mm² and a thickness of 200 µm were used as workpiece. The roughness of the workpiece was Sa = 236.1 nm with rolling texture before embossing. The workpiece was formed directly on the die without a gap or resulting flight phase of the workpiece. Hence, higher electromagnetic coupling of the die and less mechanical impact and thereby less influence on the embossing result by mechanical properties of the dies were realized.

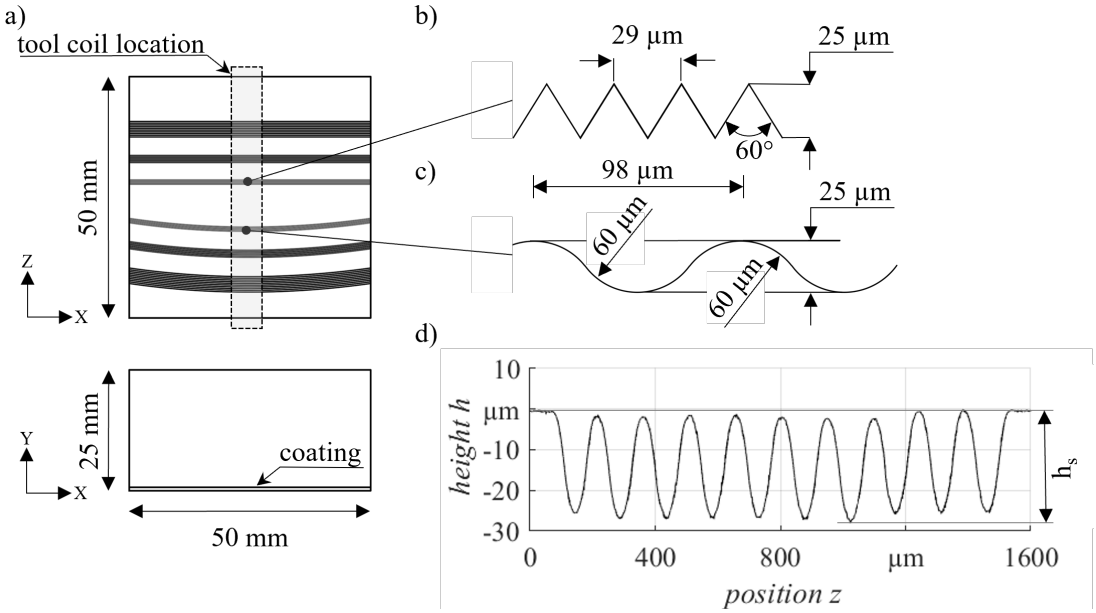

Fig. 2: Embossing die geometry a) macro geometry b) sketch of the v-groove microstructure c) sketch of the radius microstructure d) measured unfiltered radius microstructure (400 µm electroless nickel-phosphorus with 90MnCrV8-substrate)

The embossing die consisted of different v-groove structures and radius structures (see Fig. 2 a). Due to the optical effects during the optical height measurement of the v-groove, the radius microstructures with a radius of 60 µm, a height of h_s = 25 µm and 9 repetitions (see Fig. 2 b, c) were evaluated. The radius structure was produced by out-of-axis diamond turning at a mean radius of 150 mm. V-groove structures were manufactured by fly cutting with a v-shaped diamond tool. For

the v-groove structure, a height of h_s = 25 µm, a v-groove angle of 60° and 10 repetitions was used. To create a flat and regular surface, the die was face turned completely before structuring. Dies were provided in the variants listed in Tab. 2.

Based on the optical properties of the v-groove structure, they were observed using a scanning electron microscope (Hitachi TM3030Plus). Images were generated for the embossed v-groove and radius structures using backscattered electrons (BSE) acquisition at a voltage of 15kV. The radius structures were evaluated with a laser confocal microscope (Keyence VK-X 1000) at 50x magnification. To determine the embossing of the structure, the mean structure height $h_{m,s}$ over all 9 structure peaks after forming was measured. For this purpose, a two-dimensional profile of the surface structure was recorded, which was rectified from disturbances by a high-pass (cut-off: 0.25 mm) and low-pass (cut-off: 8 µm) filter. Based on the filtered profile, the mean structure height $h_{m,s}$ was determined. Determination of the surface was performed three times using a white light interferometer (Taylor Hobson CCI HD). Here, a low-pass filter of 80 µm was applied during the evaluation of the surface roughness *Sa*. The dies have shown comparable surface roughness *Sa* in the optical range (see Tab. 2).

Tab. 2: Properties of the embossing dies

substrate material	**NiP- coating** (10-12 % phosphorus)	**coating thickness s_c [µm]**	**surface roughness *Sa* [nm]** (without structures)
AlCuMgPb	no	-	5.8
90MnCrV8	yes	200	2.8
90MnCrV8	yes	400	4.3

To validate the simulation results with the performed experiments, a normalization is performed according to Eq. 4 and Eq. 5. The determined impulse $J_{y,w}$ is related to the simulated impulse with 200µm NiP layer on 90MnCrV8 substrate. Further, the determined maximum structure height h_s is related to the achieved structure height when embossing with 200 µm NiP coated 90MnCrV8 substrate.

$$\overline{J_{y,w}} = \frac{J_{y,w}}{J_{y,w}^{200\ \mu m\ NiP\ +\ 90MnCrV8}} \tag{4}$$

$$\overline{h_{m,s}} = \frac{h_{m,s}}{h_{m,s}^{200\ \mu m\ NiP\ +\ 90MnCrV8}} \tag{5}$$

Results

Simulation. The NiP-coated die used in the simulation lowered the impulse on the workpiece $J_{y,w}$ in contrast to embossing with a die with complete neutral electromagnetic properties ($\sigma = 0\ ^1/_{\Omega m}$, $\mu_r = 1$). However, this effect decreased with increasing sheet metal thickness s_0 (see Fig. 3) due to shielding and the propagation of the electromagnetic field in the sheet metal. The mark shows the penetration depth $p_{Al99.5}$ into the workpiece. The remaining penetration still leads to a slight decrease of forces.

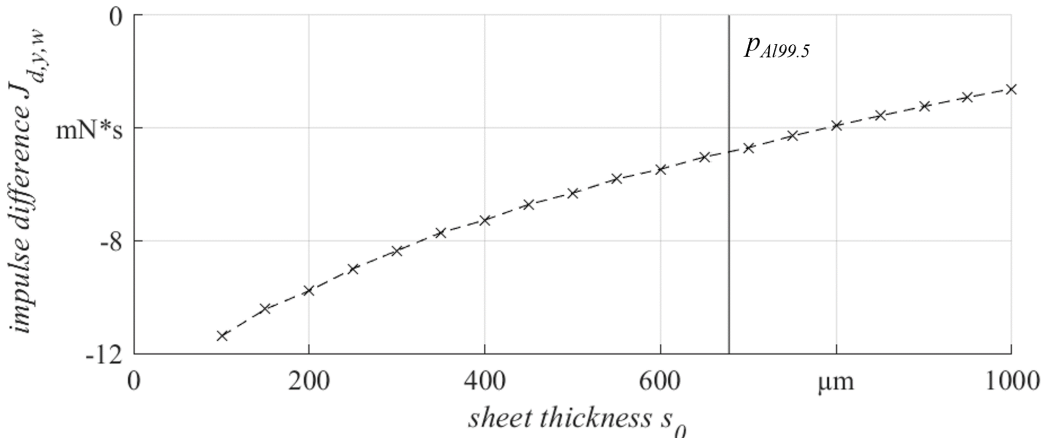

Fig. 3: Simulation of the impulse difference $J_{d,y,w}$ for an electroless nickel–phosphorus coated 90MnCrV8 substrate without relative permeability ($\sigma = 2*10^6$ $^1/_{\Omega m}$, $\mu_r = 1$) depending on the sheet metal thickness s_0 (s_c = 200 µm)

The impulse $J_{y,w}$ in electromagnetic embossing was determined for an aluminum workpiece and different coating thickness values s_c (see Fig. 4). As a reference, the horizontal lines show the values for dies without coating. Based on the shielding effect of the coating, which increases with the thickness s_c of the electroconductive coating, an influence of the electromagnetic properties of the substrate becomes apparent for coating thickness values s_c < 1400 µm. Based on the low specific resistance ρ of the aluminum (AlCuMgPb) substrate, which results in higher inducted eddy currents in the substrate that produces higher counter forces, the impulse $J_{y,w}$ in contrast to the steel (90MnCrV8) substrate is more reduced. From a coating thickness s_c of more than 1400 µm, the same impulse $J_{y,w}$ occurs independent of the substrate. This indicates that above this value, which is dependent on the electromagnetic properties of the coating, the distance between substrate, the tool coil and eddy current frequency, the electromagnetic field is completely shielded by the coating. After the complete shielding the electromagnetic properties of the coating dominate the influence of the die on the workpiece impulse $J_{y,w}$. Hence, the coating increases the die impulse $J_{y,w}$ if the electric conductivity of the substrate is higher (AlCuMgPb) and worsen if it is lower (90MnCrV8). An exception is the 100 µm thick coating on the steel substrate that enhance the performance. This case breaks the-more-the-better rule and encourages the search for optimum values.

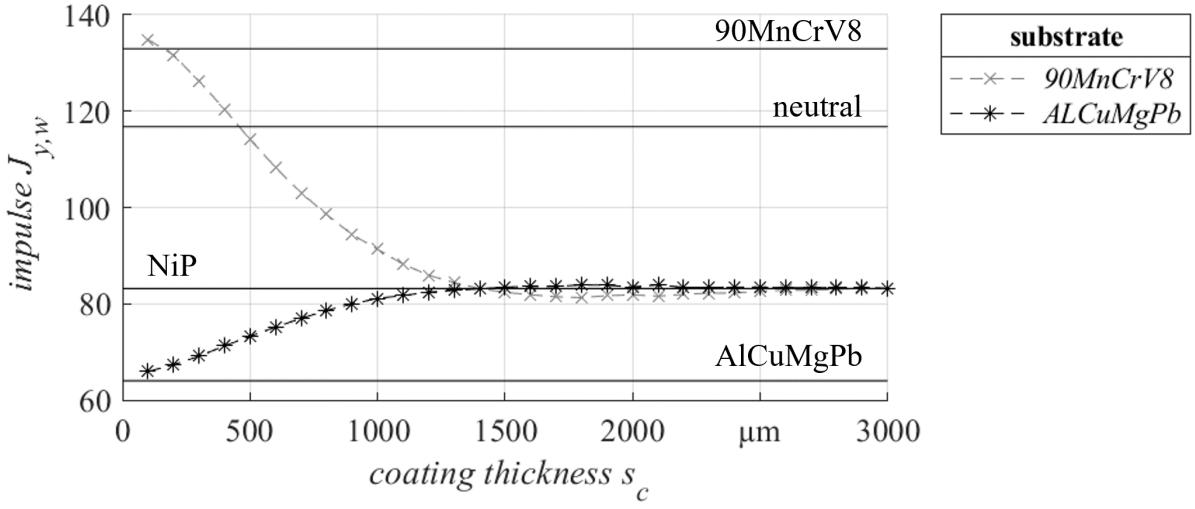

Fig. 4: Simulation of the impulse $J_{y,w}$ depending on the coating thickness s_c on 90MnCrV8 and AlCuMgPb dies; s_0= 200 µm in relation to constant values of uncoated dies from 90MnC4rV8, neutral, NiP and AlCuMgPb

In the case of complete penetration of the coating – in the varied range for s_c < 400 µm ($p_{coating,\sigma = 1*10^8\ 1/\Omega m}$) – the influence of the die on impulse $J_{y,w}$ is composed by the electromagnetic properties of substrate and coating (see Fig. 5). Basically, when varying the coating properties at constant coating thickness s_c and sheet thickness s_0, an increase in impulse $J_{y,w}$ can be assumed with increasing specific resistance ρ of the coating and substrate material. This in turn is due to the increase of induced eddy currents with low specific resistance ρ, which lead to counter forces.

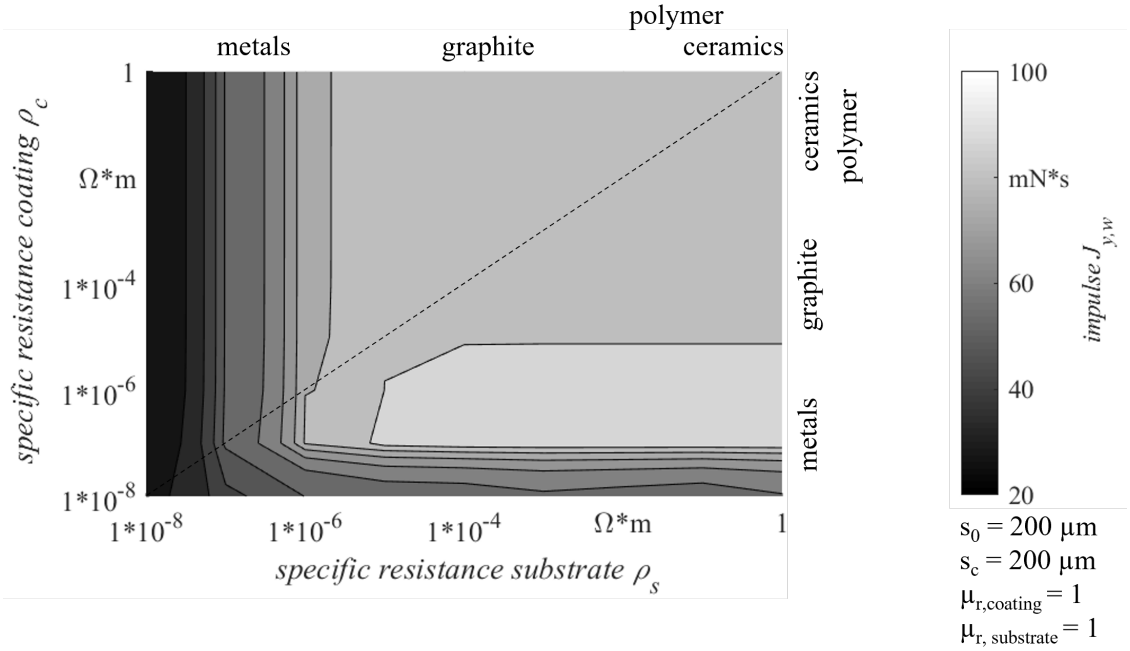

Fig. 5: Impulse $J_{y,w}$ for a variation of specific resistance ρ of coating and substrate

When coatings with high specific resistance ρ are applied, the shielding effect of the coating is not sufficient, and the property of the substrate dominates the influence on the impulse $J_{y,w}$. If coatings starting from very low specific resistance ρ are present, an increase of the impulse $J_{y,w}$ is determined until the specific resistance ρ of the workpiece is reached. Here, however the arising current in the coating reduces the impulse relatively to the neutral case, the shielding may result in a change in field propagation. Thus, flux density is locally increased, which increases the impulse $J_{y,w}$. If the specific resistance ρ of the workpiece is exceeded, the impulse $J_{y,w}$ decreases. This again can probably be explained by a change in the electromagnetic field distribution.

Experiment. An overview of the experimental embossing results is given in Fig. 6 Here, partial replication of v-groove and radius structures was achieved for all die materials except the v-grooves structures in the AlMgCuPb die. Further, the REM images show that the radius structures were replicated better than the v-groove structures. This shows that the die geometry and the resulting current density in the die influences the forming conditions. However, the embossing results clearly indicate a dependence to the die material.

The radius structure was embossed to around 10 percent in height (see Fig. 7). In comparison to a high-quality replication which was shown by Langstädtler et al. in [2], this is due to a changed tool coil and embossing without flight phase.

The lowest structure height $h_{m,s}$ was embossed by use of the aluminum die. By use of the coated dies with steel substrate, the embossing height was increased. This corresponds to the simulated impulse $J_{y,w}$. Differences based on the different coating thickness s_c cannot be determined due to the uncertainty of $h_{m,s}$. This uncertainty could be composed of the uncertainty of the measurement and the sheet roughness in relation to the microstructure size.

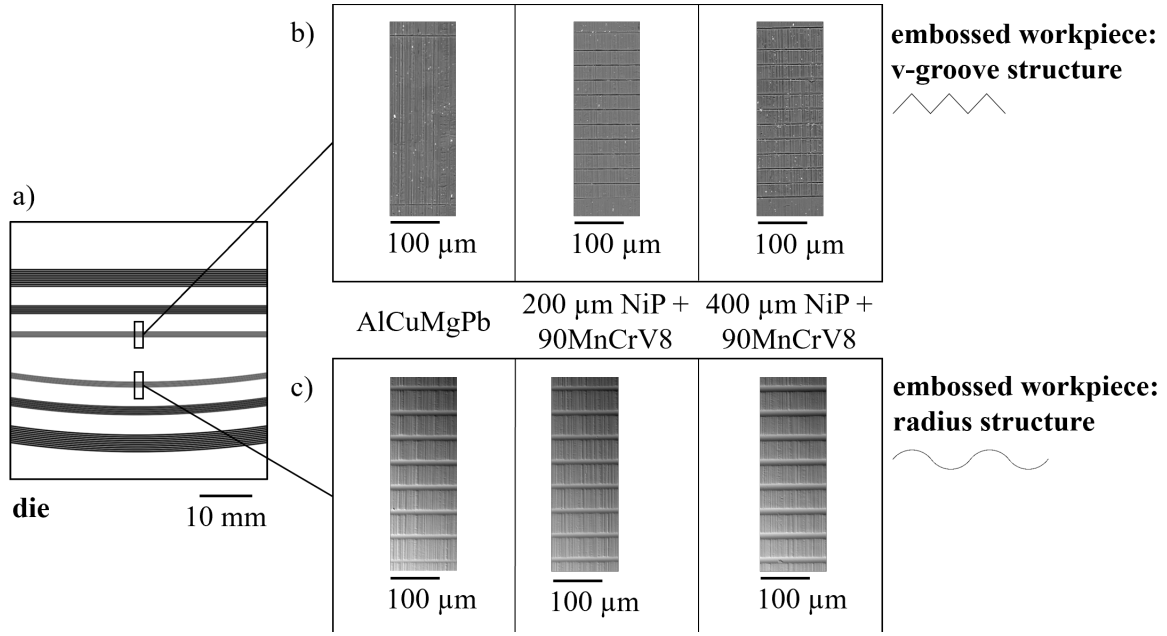

Fig. 6: REM images of embossing results a) positions of the structures on the die b) v-groove structures on Al99.5 sheet metals (s_0 = 200 µm) c) radius structures on Al99.5 sheet metals (s_0 = 200 µm)

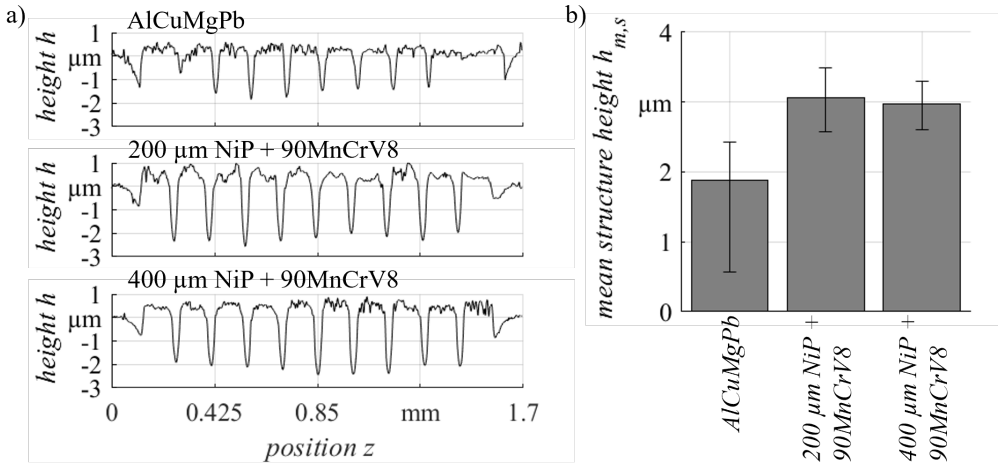

Fig. 7: Structure height for different die materials a) measured profile for different die material b) measured mean structure height $h_{m,s}$

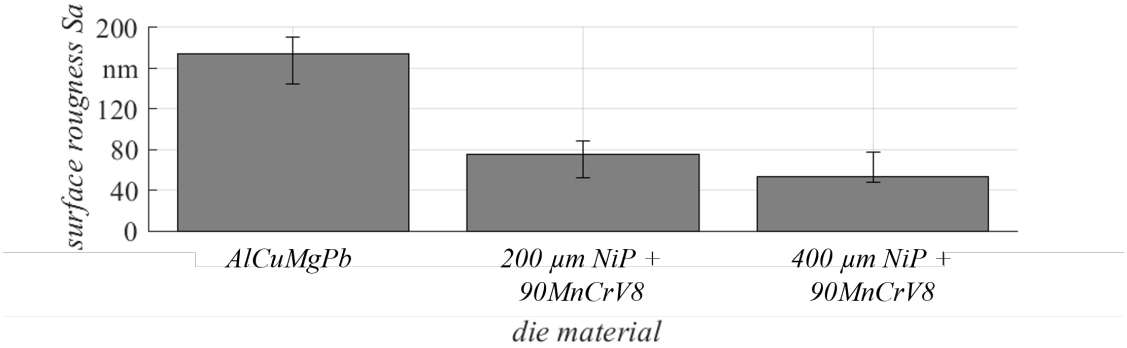

Fig. 8: Surface roughness Sa of the embossed sheet metal for different die materials

The initial surface roughness of the sheet (*Sa* = 236.1 nm) between the structures was reduced during embossing (see Fig. 8). In contrast to the two dies with steel substrate, the aluminum die shows the least amount of flattening compared to the initial sheet roughness *Sa*. This is again associated with the simulated reduced impulse $J_{y,w}$ due to the electromagnetic properties of the die. Differences due to the coating thickness s_c can again not be determined due to the uncertainty in the determination of the sheet surface roughness *Sa*.

Discussion

Coatings not only fulfill technical function like wear reduction or machinability, but clearly influence the impulse $J_{y,w}$ in electromagnetic embossing. The influence of the coating on the process due to the shielding effect must be determined as a function of sheet thickness s_0, coating thickness s_c, and applied workpiece geometry and electromagnetic properties, to enhance the process design. In addition, the changed distance between substrate and tool coil and local variations of the coating thickness through applied microstructure or by the coating process must be considered. Further, coatings and substrate may vary in their electromagnetic properties due to their production process. Therefore, the estimation of the present electromagnetic properties is difficult, so that the effect of the coating on the forming process is subject to uncertainty. In addition, electromagnetic properties depend on temperature, which changes during the forming process. Hence, resulting influences on a variation of the impulse need to be considered.

The coating and substrate can be used to affect the impulse on the workpiece and optimize the forming conditions. Optimization can be carried out with the aim of increasing the impulse $J_{y,w}$ by applying substrate and coating with increased specific resistance ρ. This is opposed by an optimization of the plastic material behavior of the workpiece according to [18, 22] which demands low specific resistance values. In addition to the electromagnetic influence, the individual mechanical properties and the influence on the process must also be considered. Here, the design in a multiple layering can also introduce the chance of separation of electromagnetic and mechanical functions to different layers.

Summary and Outlook

Within this paper, the die coating and substrate influence on the electromagnetic embossing of thin sheet metal was investigated. It was shown within two-dimensional electromagnetic field simulation that the specific resistance ρ of coating and substrate material as well as the coating thickness significantly influence the impulse $J_{y,w}$ of the workpiece and thus the embossing result. The shielding effect of the coating due to the electromagnetic properties and the distance between substrate and tool coil can lead to a dominance of the coating properties over the substrate properties for the influence on the impulse $J_{y,w}$. A low specific resistance ρ of the coating is accompanied by a high shielding effect, so there is a dominance of the coating properties. A high specific resistance ρ of the coating is accompanied by a low shielding effect, so there is a dominance of the substrate properties.

Furthermore, it was shown that a high specific resistance ρ of both, substrate and coating is attended by a high resulting impulse $J_{y,w}$ of the workpiece. In the case of low specific resistance ρ of the coating, an increase in impulse $J_{y,w}$ up to reaching the specific resistance ρ of the workpiece could be determined at high specific resistance ρ of the substrate. But in contrast to uncoated dies, the simple rule that higher specific resistance of the die causes less eddy currents and consequently lower counterforces is not fully applicable for coated dies. Further, a comparison of simulation results and embossing experiments with micro-structured aluminum and NiP-coated steel was carried out with a satisfying agreement. As a result for future work, changing the die behavior may not be limited exclusively by individual coating layers, but can include local changes in electromagnetic properties in or on the die. Accordingly, segmented and graduated layered dies are provided which, in addition to their primary function, define the forming conditions in the workpiece.

References

[1] V. Psyk, D. Risch, B.L. Kinsey, A.E. Tekkaya, M. Kleiner, Electromagnetic forming—A review, J. Mater. Process Technol. 211 (2011) 787–829.

[2] L. Langstädtler, L. Schönemann, C. Schenck, B. Kuhfuss, Electromagnetic Embossing of Optical Microstructures, J. Micro Nano-Manuf. 4 (2016) 750.

[3] S. Golowin, M. Kamal, J. Shang, J. Portier, A. Din, G.S. Daehn, J.R. Bradley, K.E. Newman, S. Hatkevich, Application of a Uniform Pressure Actuator for Electromagnetic Processing of Sheet Metal, J. Mater. Eng. Perform. 16 (2007) 455–460.

[4] J. Heidhoff, B. Beckschwarte, O. Riemer, L. Schönemann, M. Herrmann, C. Schenck, B. Kuhfuss, Electromagnetic Embossing of Optical Microstructures with High Aspect Ratios in Thin Aluminum Sheets, 24th International Conference on Material Forming (ESAFORM 2021), ULiège 14-16 April 2021.

[5] M. Herrmann, B. Beckschwarte, H. Hasselbruch, J. Heidhoff, C. Schenck, O. Riemer, A. Mehner, B. Kuhfuss, Diamond-Like-Carbon Coated Dies for Electromagnetic Embossing, Materials 13 (2020).

[6] M. Kamal, J. Shang, V. Cheng, S. Hatkevich, G.S. Daehn, Agile manufacturing of a micro-embossed case by a two-step electromagnetic forming process. J. Mater. Process. Technol. 190 (2007) 41–50.

[7] V. Psyk, C. Beerwald, A. Henselek, W. Homberg, A. Brosius, M. Kleiner, Integration of Electromagnetic Calibration into the Deep Drawing Process of an Industrial Demonstrator Part, Key. Eng. Mater. 344 (2007) 435–442.

[8] D. Risch, E. Vogli, I. Baumann, A. Brosius, C. Beerwald, W. Tillmann, M. Kleiner, Aspects of Die Design for the Electromagnetic Sheet Metal Forming Process, 2nd international conference on high speed forming, Dortmund, 20-21 March 2006.

[9] W. Tillmann, E. Vogli, Multilayers Design for the Electromagnetic Sheet Metal Forming Die, Adv. Eng. Mater. 10 (2008) 79–84.

[10] E. Vogli, F. Hoffmann, J. Nebel, D. Risch, A. Brosius, W. Tillmann, A.E. Tekkaya, Novel Layers for Dies Used in Electromagnetic Sheet Metal Forming Processes, 3rd International Conference on High Speed Forming, Dortmund 11-12 March 2008.

[11] E. Brinksmeier, W. Preuss, Micro-machining, Philos. Trans. R. Soc. A. 370 (2012) 3973–3992.

[12] D. Birdsall, F. Ford, H.P. Furth, R. Riley, Magnetic forming! Am. Mach. 105 (1961) 117–121.

[13] D. Risch, C. Beerwald, A. Brosius, M. Kleiner, On the Significance of the Die Design for Electromagnetic Sheet Metal Forming, 1st International Conference on High Speed Forming, Dortmund, 31 April 2004.

[14] Q. Cao, Z. Li, Z. Lai, Z. Li, X. Han, L. Li, Analysis of the effect of an electrically conductive die on electromagnetic sheet metal forming process using the finite element-circuit coupled method, Int. J. Adv. Manuf. Technol. 101 (2019) 549–563.

[15] Z. Lai, Q. Cao, B. Zhang, X. Han, Z. Zhou, Q. Xiong, X. Zhang, Q. Chen, L. Li, Radial Lorentz force augmented deep drawing for large drawing ratio using a novel dual-coil electromagnetic forming system, J. Mater. Process. Technol. 222 (2015) 13–20.

[16] R. Chaharmiri, A.F. Arezoodar, The Effect of Stepped Field Shaper on Magnetic Pressure and Radial Displacement in Electromagnetic Inside Bead Forming: Experimental and Simulation Analyses Using MAXWELL and ABAQUS Software, J. Manuf. Sci. Eng. 139 (2017) 787.

[17] Q. Xiong, X. Zhao, H. Zhou, M. Yang, L. Zhou, D. Gao, S. Li, A triple-coil electromagnetic two-step forming method for tube fitting, Int. J. Adv. Manuf. Technol. 116 (2021) 3905–3915.

[18] B. Beckschwarte, L. Langstädtler, C. Schenck, M. Herrmann, B. Kuhfuss, Numerical and Experimental Investigation of the Impact of the Electromagnetic Properties of the Die Materials in Electromagnetic Forming of Thin Sheet Metal, J. Manuf. Mater. Process. 5 (2021) 18.

[19] R. Parkinson, Properties and applications of electroless nickel, Nickel Development Institute 1997.

[20] ANSYS, Material Database, ANSYS, 2019.

[21] M. Kleiner, C. Beerwald, W. Homberg, Analysis of Process Parameters and Forming Mechanisms within the Electromagnetic Forming Process, CIRP Ann. - Manuf. Technol. 54 (2005) 225–228.

[22] B. Beckschwarte, M. Herrmann, C. Schenck, B. Kuhfuss, Determination of Plastic Material Properties of Thin Metal Sheets under Electromagnetic Forming Conditions, 24th International Conference on Material Forming (ESAFORM 2021), ULiège 14-16 April 2021